Cimino, G. D., Gamper, H. B., Isaacs, S. T., & Hearst, J. E. (1985) *Annu. Rev. Biochem. 54*, 1151–1193.
Cimino, G. D., Shi, Y.-B., Hearst, J. E. (1986) *Biochemistry 25*, 3013–3020.
Deering, R. A., & Setlow, R. B. (1963) *Biochim. Biophys. Acta 68*, 526–534.
Fitzpatrick, J. G., Stern, R. S., & Parrish, J. A. (1982) in *Psoriasis, Proceedings of the International Symposium, 3rd* (Farber, E. M., Ed.) pp 149–156, Grune and Stratton, New York.
Fujita, H. (1984) *Photochem. Photobiol. 39*, 835–839.
Garrett-Wheeler, E., Lockard, R. E., & Kumar, A. (1984) *Nucleic Acids Res. 12*, 3405–3423.
Gasparro, F. P., Saffran, W. A., Cantor, C. R., & Edelson, R L. (1984) *Photochem. Photobiol. 40*, 215–219.
Isaacs, S. T., Shen, C.-K. J., Hearst, J. E., & Rapoport, H. (1977) *Biochemistry 16*, 1058–1064.
Isaacs, S. T., Chun, C., Hyde, J. E., Rapoport, H., & Hearst, J. E. (1982) in *Trends in Photobiology* (Helene, C.,, Charlier, M., Monternay-Carestier, Th., & Laustriat, G., Eds.) pp 279–294, Plenum, New York.
Kanne, D., Straub, K., Hearst, J. E., & Rapoport, H. (1982) *J. Am. Chem. Soc. 104*, 6754–6764.
Kao, J. P.-Y. (1984) Ph.D. Thesis, University of California.
Krainer, A., & Maniatis, T. (1985) *Cell (Cambridge, Mass.) 42*, 725–736.
Land, E. J., & Truscott, T. G. (1979) *Photochem. Photobiol. 29*, 861–866.
Maniatis, T., Fritsch, E. F., & Sambrook, J. (1982) in *Molecular Cloning*, pp 125–127, Cold Spring Harbor Laboratory, Cold Spring Harbor, NY.
Parrish, J. A., Stern, F. S., Pathak, M. A. & Fitzpatrick, J. B. (1982) in *Science of Photomedicine* (Regan, J. D., & Parrish, J. A., Eds.) pp 595–623, Plenum, New York.
Parsons, B. J. (1980) *Photochem. Photobiol. 32*, 813–821.
Peckler, S., Graves, B., Kanne, D., Rapoport, H., Hearst, J. E., & Kim, S.-H. (1982) *J. Mol. Biol. 162*, 157–172.
Rinke, J., Appel, B., Digweed, M., & Luhrmann, R. (1985) *J. Mol. Biol. 185*, 721–731.
Saffran, W. A. & Cantor, C. R. (1984) *J. Mol. Biol. 178*, 595–609.
Setyono, B., & Pederson, T. (1984) *J. Mol. Biol. 174*, 285–295.
Shi, Y., & Hearst, J. E. (1986) *Biochemistry 25*, 5895–5902.
Shi, Y., & Hearst, J. E. (1987) *Biochemistry* (following paper in this issue).
Song, P. S., & Tapley, K. J., Jr. (1979) *Photochem. Photobiol. 29*, 1177–1197.
Straub, K., Kanne, D., Hearst, J. E., & Rapoport, H. (1982) *J. Am. Chem. Soc. 103*, 2347–2355.
Thompson, J. F., & Hearst, J. E. (1983) *Cell (Cambridge, Mass.) 32*, 1355–1365.
Turner, S., & Noller, H. F. (1983) *Biochemistry 22*, 4159–4164.
Van Houten, B., Gamper, H., Hearst, J. E., & Sancar, A. (1986a) *J. Biol. Chem. 261*, 14135–14141.
Van Houten, B., Gamper, H., Holbrook, S. R., Hearst, J. E., & Sancar, A. (1986b) *Proc. Natl. Acad. Sci. U.S.A. 83*, 8077–8081.
Zhen, W.-P., Jeppesen, C., & Nielsen, P. E. (1986) *Photochem. Photobiol. 44*, 47–51.

Wavelength Dependence for the Photoreactions of DNA–Psoralen Monoadducts. 2. Photo-Cross-Linking of Monoadducts†

Yun-bo Shi and John E. Hearst*
Department of Chemistry, University of California, Berkeley, Berkeley, California 94720
Received September 23, 1986; Revised Manuscript Received February 3, 1987

ABSTRACT: The photoreactions of HMT [4′-(hydroxymethyl)-4,5′,8-trimethylpsoralen] monoadducts in double-stranded DNA have been studied with complementary oligonucleotides. The HMT was first attached to the thymidine residue in the oligonucleotide 5′-GAAGCTACGAGC-3′ as either a furan-side monoadduct or a pyrone-side monoadduct. The HMT-monoadducted oligonucleotide was then hybridized to the complementary oligonucleotide 5′-GCTCGTAGCTTC-3′ and irradiated with monochromatic light. In the case of the pyrone-side monoadducted oligonucleotide, photoreversal was the predominant reaction, and very little cross-link was formed at all wavelengths. The course of the photoreaction of the double-stranded furan-side monoadducted oligonucleotide was dependent on the irradiation wavelength. At wavelengths below 313 nm, both photoreversal and photo-cross-linking occurred. At wavelengths above 313 nm, photoreversal of the monoadduct could not be detected, and photo-cross-linking occurred efficiently with a quantum yield of 2.4×10^{-2}.

The use of psoralens (furocoumarins) in the medical and bioloigical fields is highly dependent upon the ability of these compounds to cross-link double-stranded nucleic acids through photoreactions with adjacent pyrimidine bases on opposite strands. The cross-link formation is well understood and occurs in three steps (Song & Tapley, 1979; Parson, 1980; Parson, 1980; Cimino et al., 1985). First, psoralens intercalate between base pairs of a double-stranded nucleic acid. Second, the intercalated psoralens photoreact with pyrimidine bases to form psoralen–pyrimidine monoadducts under UV (320–400 nm) irradiation. Finally, the monoadducts photoreact with adjacent pyrimidine bases by absorbing a second photon to form diadducts that cross-link the two strands of the nucleic acid together. It has been well established that the furan-side monoadduct can be easily driven to a diadduct in a double-

† This work was supported by NIH Grant GM11180.
* Author to whom correspondence should be addressed.

0006-2960/87/0426-3792$01.50/0

stranded nucleic acid. Gasparro et al. (1984) have reported the action spectrum for the AMT [4′-(aminomethyl)-4,5′,8-trimethylpsoralen] cross-linking of pBR322 DNA in the wavelength region from 300 to 380 nm. They found that the wavelength dependence for cross-link formation correlates with the absorption spectrum of the furan-side monoadduct. Tessman et al. (1985) have reported the photo-cross-linking of another furan-side monoadduct, thymidine–8-methoxypsoralen furan-side monoadduct, in calf thymus DNA. They observed that the monoadduct could be converted to the diadduct at 341.5 nm with a quantum yield of 2.8×10^{-2}. The pyrone-side monoadducts do not absorb light above 320 nm, so they cannot be driven to diadducts with 320–380-nm light.

In the preceding paper (Shi & Hearst, 1987), we reported the wavelength dependence for the photoreversals of DNA–HMT monoadducts [HMT: 4′-(hydroxymethyl)-4,5′,8-trimethylpsoralen][1] and isolated T–HMT monoadducts. We found that both the DNA–HMT and the T–HMT pyrone-side monoadducts are photoreversible at wavelengths below 334 nm, which is consistent with the absorption spectrum of the T–HMT pyrone-side monoadduct. The DNA–HMT and T–HMT furan-side monoadducts can be photoreversed at wavelengths up to 365 nm, which also correlates with the absorption spectrum of the T–HMT furan-side monoadduct. The quantum yield of the photoreversal of the furan-side monoadduct is, however, only 7×10^{-4} at wavelengths above 285 nm, which is much smaller than the photo-cross-linking quantum yield of the thymidine–8-methoxypsoralen furan-side monoadduct at 341.5 nm as reported by Tessman et al. (1985). Here we report the complete action spectra for the photoreactions of DNA–HMT monoadducts in a double-stranded helix. We observed that the DNA–HMT pyrone-side monoadduct yielded very little cross-link and was predominantly photoreversed upon UV irradiation in its absorption bands. In the case of the DNA-HMT furan-side monoadduct, UV irradiation at wavelengths ≥313.2 nm yields only cross-link with a quantum yield similar to that observed by Tessman et al. (1985), whereas UV irradiation at wavelengths ≤302.2 nm yields both photo-cross-linking and photoreversal products.

Materials and Methods

Materials. All materials were obtained as described in the preceding paper (Shi & Hearst, 1987).

Preparation of 5′-End Labeled DNA Oligonucleotides. The DNA oligonucleotides used in this study are 5′-GAAGCTACGAGC-3′, 5′-GCTCGTAGCTTC-3′, and 5′-TCGTAGCT-3′, respectively called oligonucleotide A, B, and C. The furan-side DNA–HMT monoadduct, 5′-GAAGC[T-(HMT)$_{Fu}$]ACGAGC-3′ (M_{Fu}-A), and the pyrone-side DNA–HMT monoadduct, 5′-GAAGC[T(HMT)$_{Py}$]ACGAGC-3′ (M_{Py}-A), were prepared as described in the preceding paper (Shi & Hearst, 1987). All unmodified and HMT-monoadducted oligonucleotides were 5′-phosphorylated. Oligonucleotides with 5′-OH were labeled with [γ-^{32}P]ATP and T4 polynucleotide kinase and subsequently chased with cold ATP (Maniatis et al., 1982; Shi & Hearst, 1986). The kinase exchange reaction was used to label oligonucleotides with 5′-phosphate (Maniatis et al., 1982; Shi & Hearst, 1987).

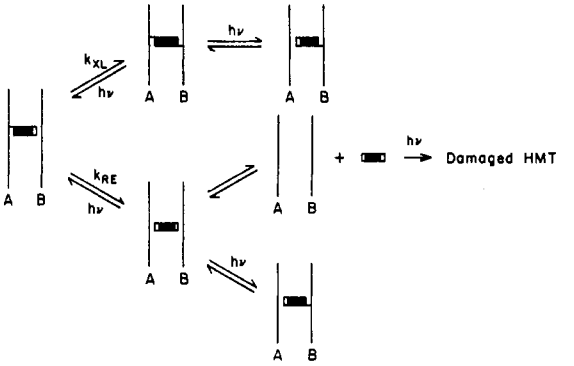

FIGURE 1: Photoreaction kinetics of HMT monoadducts in double-stranded DNA.

The concentrations of the unmodified and HMT-monoadducted DNA oligonucleotides were determined by absorption measurements at 260 nm. The extinction coefficients for oligonucleotides A–C and M_{Fu}-A and M_{Py}-A are 1.2×10^5, 1.1×10^5, 7.4×10^4, 1.3×10^5, and 1.3×10^5, respectively (Shi & Hearst, 1986).

Photo-Cross-Linking of the DNA–HMT Monoadducts. Monochromatic irradiations were done with the apparatus as described by Cimino et al. (1986). The bandwidth was maintained constant at 5.0 nm. The light intensity was monitored continuously with an in-line photoiode, which was calibrated by actinometry with $K_3Fe(C_2O_4)_3$. The photo-cross-linking of the DNA–HMT monoadducts, both M_{Fu}-A and M_{Py}-A, was done in the presence of the cold 5′-phosphorylated complementary oligonucleotide B or C. The solutions were irradiated with monochromatic light in a stirred cuvette, which was covered with Parafilm, at 4 °C in 100 mM NaOAc, 10 mM $MgCl_2$, and 0.1 mM EDTA, pH 6.0, or as otherwise indicated. A total of 16 μg of carrier tRNA was added to each sample after irradiation, and the sample was then concentrated in a Speedvac concentrator (Savant Instrument Inc.) to 400 μL (irradiation volume was 750 μL) and EtOH precipitated overnight (2.5 v/v EtOH) at −20 °C. The sample pellets were then dissolved in 8 M urea, 0.02% bromophenol blue, and 0.02% xylene cyanol FF loading buffer and electrophoresed on a 20° polyacrylamide–7 M urea gel (40 cm × 40 cm × 0.05 cm, 35 W for 3–4 h). Band positions of the photoproducts and the reactants were located by autoradiography. The bands were then excised and quantified by ^{32}P Cerenkov counting with a Beckman LS-230 liquid scintillation counter.

Kinetics of the Photoreactions. The photoreactions of DNA–HMT monoadducts in double-stranded DNA are relatively complicated. Figure 1 shows the possible reactions of a double-stranded DNA formed between oligonucleotides A and B, with an HMT monoadduct attached to A. The initial reactions are the photoreversal and the photo-cross-linking of the monoadduct. Photo-cross-linking yields a cross-link that links A and B together. Upon absorbing a second photon, the cross-link can be photoreversed to yield a DNA–HMT monoadduct with the HMT attached to either B or A. photoreversal of the monoadduct gives a complex with the HMT molecule intercalated in the double-stranded helix A:B. This complex can undergo either a photoreaction to yield a DNA–HMT monoadduct or a reversible dark dissociation to yield a free HMT molecule, which can be subsequently photodamaged.

Instead of relying upon the complicated kinetic equations, we used initial rate analysis to obtain the rate constants for the photoreversal and photo-cross-linking of the monoadducts.

[1] Abbreviations: HMT, 4′-(hydroxymethyl)-4,5′,8-trimethylpsoralen; EtOH, ethanol; ATP, adenosine 5′-triphosphate; EDTA, ethylenediaminetetraacetic acid; Tris, tris(hydroxymethyl)aminomethane; M_{Fu}, furan-side monoadduct; M_{Py}, pyrone-side monoadduct; 5′-[T-(HMT)$_{Fu}$]-3′, thymidine–HMT furan-side monoadduct with HMT on the 3′-side of the thymidine; 5′-[T(HMT)$_{Py}$]-3′, thymidine–HMT pyrone-side monoadduct with HMT on the 3′-side of the thymidine; T–HMT–T, thymidine–HMT–thymidine diadduct.

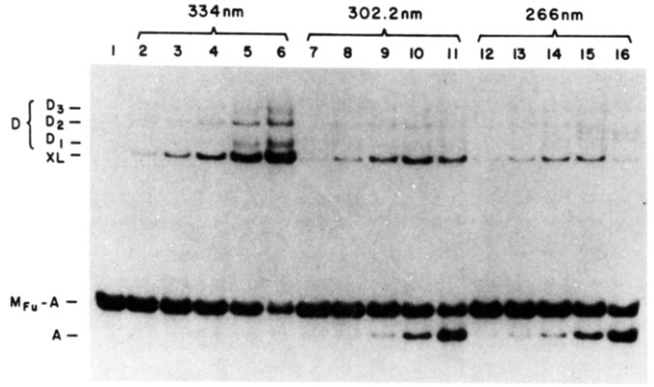

FIGURE 2: Photo-cross-linking of double-stranded M_{Fu}-A:B. $V = 750$ μL; $l = 1$ cm. Abbreviations: A = 5′-GAAGCTACGAGC-3′; M_{Fu}-A = 5′-GAAGC[T(HMT)$_{Fu}$]ACGAGC-3′; B = 5′-GCTCGTAGCTTC-3′; XL = cross-link formed between M_{Fu}-A and B through the addition of the pyrone end of the HMT to the middle thymidine in B; D_1, D_2, and D_3 = XL with DNA damage(s) (see text). (Lane 1) Dark control; (lane 2–6) samples exposed to 2.37×10^{16}, 5.28×10^{16}, 1.06×10^{17}, 3.20×10^{17}, and 1.07×10^{18} photons at 334 nm, respectively. Light intensity was 1.58×10^{15} photons/s for lane 2 and 3.56×10^{15} photons/s for the other lanes. (Lanes 7–11) Samples exposed to 5.52×10^{16}, 1.29×10^{17}, 3.43×10^{17}, 1.03×10^{18}, and 3.54×10^{18} photons at 302.2 nm, respectively. Light intensity was 3.68×10^{15} photons/s for lane 7 and 8.58×10^{15} photons/s for the other lanes. (Lanes 12–16) Samples exposed to 1.49×10^{16}, 2.99×10^{16}, 7.97×10^{16}, 2.49×10^{17}, and 7.97×10^{17} photons at 266 nm, respectively. Light intensity was 1.66×10^{14} photons/s.

The photoreaction kinetics at very low reactant concentrations can be analyzed as described by Cimino et al. (1986) to obtain the following initial rate equations:

$$-\mathrm{d}(C/C^0)/\mathrm{d}(I_0t) = lk_t/(VN_0) \quad (1)$$

$$\mathrm{d}(P/C^0)/\mathrm{d}(I_0t) = lk/(VN_0) \quad (2)$$

$$k = 2.303\epsilon\phi \quad (3)$$

where k_t is the total photoreaction rate constant of the DNA–HMT monoadduct [L/(einstein·cm)] I_0 is the light intensity (photons/s), I_0t is the irradiation dose (photons), V is the reaction volume (L), N_0 is Avogardro's number, L is the path length (cm), ϵ is the extinction coefficient of the monoadduct; P is the concentration of a product, k and ϕ are the rate constant [L/einstein·cm)] and the quantum yield for the formation of P, respectively, and C^0 and C are the concentrations (mol/L, or M) of the DNA–HMT monoadduct at time zero and at time t, respectively.

RESULTS

Photo-Cross-Linking of 5′-GAAGC[T(HMT)$_{Fu}$]-ACGAGC-3′. The photo-cross-linking of M_{Fu}-A (2 nM) was done in the presence of a 10–fold excess (20 nM) of its unlabeled complementary oligonucleotide B (5′-GCTCGTAGCTTC-3′) at 4 °C in 100 mM NaOAc, 10 mM $MgCl_2$, and 0.1 mM EDTA, PH 6.0. Under these conditions, M_{Fu}-A and its complement B exist in the double-stranded state (Shi & Hearst, 1986). The photo-cross-linking samples were irradiated with monochromatic light followed by EtOH precipitation in the presence of carrier tRNA. The samples were then electrophoresed on a 20% polyacrylamide gel to separate the photoproducts. An autoradiogram of the time course of the irradiation at three wavelengths is shown in Figure 2. With increasing dose, the amount of M_{Fu}-A decreased at all wavelengths. Product formation is very dependent on the irradiation wavelength. The three wavelengths in the figure are in three different absorption bands of the isolated T–HMT furan-side monoadduct [see Figure 3 of the preceding paper (Shi & Hearst 1987)]. More photoreversal product (A) was produced at shorter wavelengths. No photoreversal occurred at 334 nm. More cross-link(s), which link(s) the oligonucleotides A and B together through the middle thymidine on each strand, was (were) produced at longer wavelengths. The bands moving slower than the cross-link XL, i.e., D_1, D_2, D_3, were identified as cross-links with photodamage(s) on oligonucleotide B and/or A (see below). At 334 nm, XL and D (including D_1, D_2, and D_3) increased with increasing dose, whereas at shorter wavelength(s) XL and D increased first and then decreased with increasing dose. This is attributed to the competing photoreversal of the cross-links at the shorter wavelengths since it is known that cross-links can be photoreversed at wavelengths ≤313 nm (Cimino et al., 1986). It is also apparent that the damaged cross-link formation is dependent upon the wavelength and that more damaged bands were seen at 266 nm.

The identities of the photoproducts were tested by the following experiments. Unlabeled M_{Fu}-A and ^{32}P-labeled B were irradiated under the same conditions as above and then analyzed by gel electrophoresis. Again, the cross-linking yielded XL, D_1, D_2, and D_3. Upon photoreversal at 254 nm, these purified adducts yielded, as expected, M_{Py}-B and B as analyzed by gel electrophoresis. These and above results indicate that XL, D_1, D_2, and D_3 are DNA–HMT cross-links. In addition, photoreversal of D_2 and D_3 yielded bands running slightly slower than B. When similar photoreversal was performed on XL, D_1, D_2, and D_3 with labeled A strand, only A and M_{Fu}-A were produced in all cross-links. These results suggest that there is photodamage on the B strand in D_2 and D_3. But the possibility that damage on the A strand, especially in the case of D_1 where photoreversal yielded no damaged DNA when the label was on either A strand or B strand, cannot be ruled out because of the possibility of photoreversal of the damage at 254 nm, especially pyrimidine dimers, and the limited resolution by gel electrophoresis. The mechanism of the damaged product formation is unknown. These products could be produced by direct absorption of the DNA bases or more probably by energy tranfer from the excited psoralen moiety to the pyrimidine bases, especially at wavelengths ≥334 nm, where DNA bases have little absorption. It has been shown that the triplet states of the furan-side monoadducts of several psoralen derivatives with thymine as well as those of coumarin and 4′,5′-dihydropsoralen can be quenched by nucleic acid bases (Bensasson et al., 1980; Land & Truscott, 1979; Blais et al. 1985), suggesting that energy transfer between these adducts and nucleic acid bases can occur.

The bands of the reactant and the products, such as those in Figure 2, were excised and quantified by ^{32}P Cerenkov counting in order to determine the concentration of each reactant and product. The plots of the concentrations as a function of irradiation dose at 302.2 and 334 nm are shown in Figure 3, where D stands for the total damaged cross-links running slower than XL on the gel. Again, it can be seen that only XL and D were produced at 334 nm, whereas photoreversal of M_{Fu}-A to yield A was a competing process at 302.2 nm. With increasing dose at 302.2 nm, XL and D initially increased and then decreased due to the photoreversal of the cross-links. The production of A was sigmoidal. Initially A was produced only from the photoreversal of M_{Fu}-A. As more XL and D were formed, a significant amount of A was produced from the photoreversal of XL and D, since it is known that about 30% of the time photoreversal of cross-links at this wavelength occurs at the furan end (Cimino et al., 1986), which in our case yields A. Consequently, the rate of A formation is increased. The initial rate constants for the

Table I: Initial Rate Constants of M_{Fu}-A Cross-Linking[a]

	λ = 248 nm			λ = 297 nm			λ = 334 nm		
	25 °C,	4 °C		25 °C,	4 °C		25 °C,	4 °C	
	B	B	C	B	B	C	B	B	C
k^t	2020	2530	2010	285	321	212	680	1050	529
k^t_{XL}	870	1090	740	266	280	173	680	1050	529
k_{RE}	1150	1440	1270	19	41	39	0	0	0
k_D/k^t_{XL}	0.43	0.51	0	0.37	0.54	0	0.29	0.44	0

[a] Abbreviations: M_{Fu}-A = 5′-GAAGC[T(HMT)$_{Fu}$]ACGAGC-3′; B = 5′-GCTCGTAGCTTC-3′; C = 5′-TCGTAGCT-3′. Irradiation buffer: 100 mM NaOAc, 10 mM $MgCl_2$, and 0.1 mM EDTA, pH 6.0. Concentrations: [M_{Fu}-A] = 2 nM; [B] = 20 nM; [C] = 6 nM. k^t is total photoreaction rate constant of M_{Fu}-A [L/(einstein·cm)]; k^t_{XL} is total photo-cross-linking rate constant [L/(einstein·cm)]; k_{RE} is photoreversal rate constant [L/(einstein·cm)]; k_D is rate constant of damaged cross-link formation [L/(einstein·cm)]. Estimated precision in rate constants is ±20%.

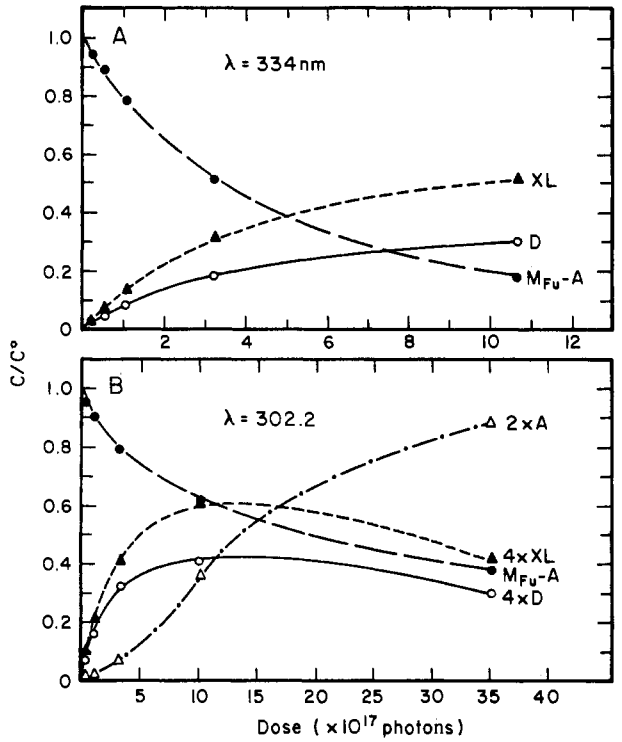

FIGURE 3: (A) C/C^0 vs. irradiation dose for the photo-cross-linking of M_{Fu}-A. All the irradiation conditions and abbreviations are identical with those described in Figure 2. The ratios of concentrations of the reactant (M_{Fu}-A) and the products (A, XL, and D) to the initial concentration of M_{Fu}-A plotted in this figure were determined by excising the bands from the photo-cross-linking gel and measuring the ^{32}P counts of each band with a scintillation counter. The relative concentrations of A, XL, and D shown in (B) are the actual value for each product multiplied respectively by 2, 4, and 4 as indicated in the figure for the convenience of presentation.

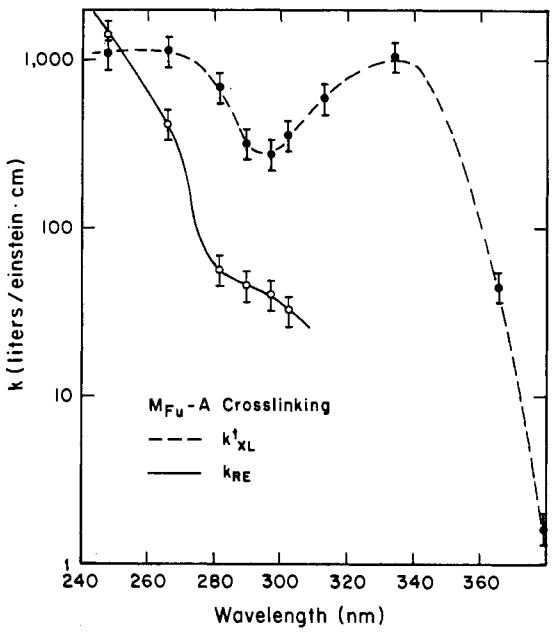

FIGURE 4: Action spectra for the photoreversal and photo-cross-linking of T–HMT furan-side monoadduct in double-stranded M_{Fu}-A:B. k^t_{XL} is the initial rate constant for the total cross-link formation, and k_{RE} is the initial rate constant for the formation of the unmodified oligonucleotide A, i.e., the photoreversal. k_{RE} is zero at wavelengths ≥313 nm.

photoreversal (k_{RE}) and for XL and D formation (k_{XL} and k_D, respectively) were determined from these plots. The experiments were repeated at wavelengths ranging from 248 to 379 nm to obtain the action spectra for the photoreversal and photo-cross-linking. Figure 4 shows the initial rate constants for the photoreversal (k_{RE}) and the total cross-link formation ($k^t_{XL} = k_{XL} + k_D$) as a function of wavelength. Essentialy no initial photoreversal occurs at wavelengths ≥313 nm, although a detectable amount of A was produced after prolonged irradiation at 313.2 nm, which was due to photoreversal of the cross-link (Cimino et al., 1986).

Two series of experiments were done to determine the dependence of the reaction rate on the stability of the double helix. In the first, the irradiation temperature was raised from 4 to 25 °C, and in the second, the oligonucleotide C was used as the complement of M_{Fu}-A. The photoreaction data were analyzed as described above, and the results are presented inTable I. When the irradiation temperature was changed from 4 to 25 °C without altering other conditions, the photoreaction rate constants were slightly decreased, though the differences were not significant compared to the experimental error (see data in the first and second columns for each wavelength). The ratio of k_D/k^t_{XL} at 25 °C was also smaller than that at 4 °C at all wavelengths, indicating that fewer damaged cross-links (D) were produced at the higher temperature. Data in the second and third columns for each wavelength show that the rate constants when C was used as the complement were smaller than those obtained with B as the complement. The results from these two series of experiments indicate that the photoreactions are less efficient in less stable helices. Also shown by these experiments is that the ratio of k_D/k^t_{XL} was 0, or no damaged cross-links (D) were produced, at all wavelengths when C was used as the complement.

To ensure that all M_{Fu}-A were in double-stranded state under the conditions used to obtain the action spectra shown in Figure 4, the salt concentration of the irradiation buffer and/or the DNA concentrations were increased, and the samples were irradiated at 334 nm and analyzed as described above. The results are shown in Table II. Upon changing the $MgCl_2$ concentration in the irradiation buffer from 10 to 20 mM or increasing the DNA concentrations by a factor of five, or both, the photoreversal rate constants as well as the ratio of k_D/k^t_{XL} remained the same. Since these changes favor double-stranded DNA formation, the results indicate that

Table II: Initial Rate Constants at 334 nm and 4 °C[a]

	sample set			
	1	2	3	4
$[M_{Fu}\text{-A}]$ (nM)	2	10	2	10
[B] (nM)	20	100	20	100
buffer	B1	B1	B2	B2
$k^t = k^t_{XL}$	1050	1010	1040	1000
k_D/k^t_{XL}	0.44	0.44	0.37	0.42

[a] Abbreviations: See Table I. Buffers: B1 = 100 mM NaOAc, 10 mM $MgCl_2$, and 0.1 mM EDTA, pH 6.0; B2 = 100 mM NaOAc, 20 mM $MgCl_2$, and 0.1 mM EDTA, pH 6.0. Estimated precision in rate constants ±20%.

under the original conditions all the M_{Fu}-A was double-stranded.

Tessman et al. (1985) have reported that a thymidine–8-methoxypsoralen furan-side monoadduct in double-stranded calf thymus DNA can be converted to a pyrone-side monoadduct by direct photoisomerization upon irradiation at 341.5 nm. To test whether the T–HMT furan-side monoadduct in a double helix can photoisomerize to the pyrone-side monoadduct, 5′-^{32}P-labeled oligonucleotide C was used as the complement of M_{Fu}-A in photo-cross-linking experiments. Any production of pyrone-side monoadducted C could be detected as a unique band on a polyacrylamide gel (Shi & Hearst, 1986). These experiments showed that no pyrone-side monoadducted C was produced at 334 nm, although detectable amounts were generated at 297 and 248 nm. Formation of M_{Py}-C at shorter wavelengths was probably due to the photoreversal of the cross-link formed in the forward cross-linking reaction. Therefore, it is concluded that the T–HMT furan-side monoadduct cannot undergo direct photoisomerization. The difference between this adduct and the thymidine–8-methoxypsoralen furan-side monoadduct is probably due to the nature of the two psoralen derivatives.

The reciprocity of the photoreactions was confirmed by exposing several identical samples to a constant light dose (1.08×10^{17} photons) at 334 nm. The light intensity seen by each sample was varied by up to a factor to ten, and the irradiation time was varied correspondingly to maintain the constant dose. The photoreactions in all samples occurred to the same extent. They are, therefore, dependent only on the irradiation dose and not on the light intensity and are one-photon processes. The initial rate constants determined above should also be independent of light intensity.

The quantum yield of initial cross-link formation was estimated on the basis of k^t_{XL} and the extinction coefficient of the isolated T–HMT furan-side monoadduct [Figure 3 of the preceding paper (Shi & Hearst 1987)] according to eq 3. The result is shown in Table III. The quantum yield in the shorter wavelength region is slightly larger than that in the longer wavelength region. The quantum yield above 300 nm is 2.4×10^{-2}, which is similar to that reported by Tessman et al. (1985) for the cross-linking of thymidine–8-methoxypsoralen furan-side monoadduct in calf thymus DNA. The uncertainty in quantum yield is not known due to the unknown effects that the DNA helix and bases may have on the absorption of the T–HMT furan-side monoadduct in the double-stranded M_{Fu}-A:B helix, especially in the wavelength regions where

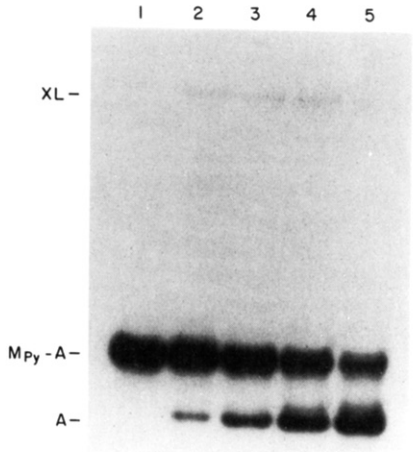

FIGURE 5: Photo-cross-linking of double-stranded M_{Py}-A:B. $V = 750$ μL; $l = 1$ cm. Abbreviations: M_{Py}-A = 5′-GAAGC[T(HMT)$_{Py}$]-ACGAGC-3′; XL = cross-link formed between M_{Py}-A and B through the addition of the furan end of the HMT to the middle thymidine in B. (Lane 1) Dark control; (lanes 2–5) samples exposed to 2.33×10^{17}, 7.0×10^{17}, 2.10×10^{18}, and 7.0×10^{18} photons at 297 nm, respectively. Light intensity was 5.83×10^{15} photons/s.

DNA bases absorb. Energy transfer from excited DNA bases to the HMT group may also contribute to the cross-linking, which may explain the bigger quantum yield around 260 nm.

Photo-Cross-Linking of 5′-GAAGC[T(HMT)$_{Py}$]-ACGAGC-3′. The photo-cross-linking of M_{Py}-A (2 nM) was performed under the same conditions used for M_{Fu}-A. All of the M_{Py}-A should be double stranded under these conditions on the basis of the thermodynamic parameters for the double-helix formation by M_{Py}-A and B (Shi & Hearst, 1986). The photo-cross-linking samples were treated as above, and an autoradiogram of the time courses of the irradiation at 297 nm is shown in Figure 5. With increasing irradiation dose, the amount of M_{Py}-A decreased. The loss of M_{Py}-A was predominantly photoreversal. The amount of XL formed was only a few percent, and it decreased after prolonged irradiation (compare lane 5 to lanes 2–4). When this XL was isolated and photoreversed at 254 nm, it gave M_{Py}-A and A (data not shown), indicating that in XL the HMT is attached to A through its pyrone end and attached to B through its furan end and that the formation of XL was not due to contamination of M_{Py}-A with M_{Fu}-A. The bands migrating slightly slower than A represent damaged DNA. These same bands were also observed in the photoreversal of M_{pY}-A in its single-stranded state [see the preceding paper, (Shi & Hearst, 1987)]. The amount of material in each band was quantified by excising the band from the gel and counting it in a scintillation counter. The photoreaction rate constant(s) could then be determined. The experiments were repeated at different wavelengths in both absorption bands of the T–HMT pyrone-side monoadduct [see Figure 4 of the preceding paper (Shi & Hearst, 1987)]. It was found that photoreversal was the predominant reaction and that only a few percent of XL was formed at all wavelengths. Thus, the total photoreaction rate constant (i.e., the rate constant for the consumption of M_{Py}-A) is approximately equal to the photoreversal rate constant of M_{Py}-A in the double-stranded helix. The photo-

Table III: Quantum Yield of M_{Fu}-A Cross-Linking[a]

	λ (nm)								
	248	266	281.7	289.5	297	302.2	313.2	334	365.4
ϕ ($\times 10^{-2}$)	5	8	4	2	1.2	1.4	1.7	2.4	4

[a] Oligonucleotide B was used as the complement in the photoreaction (4 °C). See Table I for abbreviations and other reaction conditions.

Table IV: Photoreaction Rate Constant of M_{Py}-A[a]

	λ = 248 nm				λ = 297 nm			
	4 °C, buffer B1			24 °C, buffer B3, no complement	4 °C, buffer B1			24 °C, buffer B3, no complement
	B	C	no complement		B	C	no complement	
k^t	1980 ± 270	1640 ± 180	917 ± 92	731 ± 73	116 ± 19	97 ± 21	52 ± 5	45 ± 5[b]

[a] Abbreviations: M_{Py}-A = 5′-GAAGC[T(HMT)$_{Py}$]ACGAGC-3′ and see Table I. Buffers: B1 = 100 mM NaOAc, 10 mM $MgCl_2$, and 0.1 mM EDTA, pH 6.0; B3 = 0.1 mM EDTA, pH 5.5. Concentrations: [M_{Py}-A] = 2 nM; [B] = 20 nM; [C] = 10 nM. k^t is total photoreaction rate constant of M_{Py}-A [L/(einstein·cm)]. [b] Data from the preceding paper (Shi & Hearst, 1987).

reaction rate constants at 248 and 297 nm under these conditions are listed in the first column for each wavelength in Table IV. Compared to the photoreversal rate constant of the single-stranded M_{Py}-A in the fourth column for each wavelength, the photoreversal rate in a double-stranded helix is about twice as fast as that in a single-stranded helix. The enhancement of photoreversal under the photo-cross-linking conditions could be due to (1) photoreversal through a transient photo-cross-linking, i.e., through formation and photoreversal of XL, which would give mostly oligonucleotide A and M_{Fu}-B (Cimino et al., 1986), (2) direct photoisomerization, i.e., the excited HMT group photoreversing at its pyrone end and simultaneously attaching to the thymidine residue in B through its furan end, (3) the irradiation buffer and/or temperature, (4) the electronic properties and steric constraints of the pyrone-side monoadduct in the double-stranded DNA, and (5) energy transfer from excited DNA bases in double-stranded DNA to the HMT group.

The first two possibilities were investigated by irradiating samples of M_{Py}-A in the presence of ^{32}P-labeled complementary oligonucleotide C under the same conditions as above. The furan-side monoadducted C, if generated by either one of these, could be detected as a unique band on a polyacrylamide gel (Shi & Hearst, 1986). These experiments showed that the furan-side monoadducted C was generated at only a few percent even when most of the M_{Py}-A had been photoreversed. The photoreaction rate constants at 248 and 297 nm and the amount of XL formed were similar to those obtained when oligonucleotide B was used as the complement, and the rate constants are shown in the second column for each wavelength in Table IV. On the basis of all these results, it is concluded that the photoreversal through transient cross-linking and direct photoisomerization may contribute to the enhancement of the photoreversal, but they have only a small effect and cannot explain the twofold enhancement. To test the third possibility, samples of M_{Py}-A were irradiated under the same conditions as above except no complement was added and the irradiated samples were analyzed to obtain the photoreversal rate constant. These results, shown in the third column for each wavelength in Table IV, show that the photoreversal rate constant of single-stranded M_{Py}-A in the buffer at 4 °C is identicaly with that in 0.1 mM EDTA at 24 °C. Thus, the enhancement of photoreversal is dependent on double-helix formation and independent of the irradiation temperature and buffer conditions. The effects of double-stranded DNA formation on the electronic properties and the steric constraints of the pyrone-side monoadduct and the possibility of energy transfer from excited DNA bases to the HMT group cannot be directly tested.

Discussion

Effects of Double-Helix Formation on the Photoreactions of M_{Fu}-A. Photoreversal is the only reaction that occurs when single-stranded M_{Fu}-A is irradiated with UV light as described in the preceding paper. In the presence of complement B (5′-GCTCGTAGCTTC-3′) or C (5′-TCGTAGCT-3′), the photoreactions of M_{Fu}-A become more complicated. Initially, there are two parallel reactions: photoreversal and photo-cross-linking of M_{Fu}-A to its complement. The relative rate of photoreversal vs. photo-cross-linking is dependent on irradiation wavelength. As shown in Figure 4, except at wavelengths below 250 nm, photo-cross-linking is the favored reaction for the double-stranded M_{Fu}-A:B, and the ratio of k^t_{XL}/k_{RE} increases as the irradiation wavelength increases. At wavelengths ≥313 nm, only photo-cross-linking occurs. Photo-cross-linking is still detectable at 379 nm. Due to the photoreversibility of the cross-link(s), unmodified oligonucleotide A will be the major product after prolonged irradiation at wavelength ≤313 nm.

The initial photoreversal rate constant k_{RE} is larger than that for the single-stranded M_{Fu}-A as reported in the preceding paper. As for M_{Py}-A in double-stranded M_{Py}-A:B, there as several possible causes for this enhanced photoreversal, which have not been tested. The k_{RE} in Figure 4 overestimates the actual photoreversal rate constant, since cross-link formation and subsequent photoreversal are fast and 30% of this photoreversal yields unmodified oligonucleotide A (Cimino et al., 1986), which contributes to the apparent photoreversal rate.

The efficient photo-cross-linking of DNA–HMT furan-side monoadducts at wavelengths above 313 nm, where DNA bases do not absorb, enhances the usefulness of oligonucleotide hybridization probes. Cross-linkable HMT-monoadducted oligonucleotide probes facilitate solution hybridization formats, which are much more rapid and convenient than traditional hybridization methods. These same probes can be used to study hybridization kinetics and thermodynamics of the interactions between oligonucleotides and large nucleic acids (Cimino et al., submitted for publication; Gamper et al., submitted for publication).

Quantum Yield of Photo-Cross-Linking of M_{Fu}-A. The accurate quantum yield for photo-cross-linking is difficult to determine due to the difficulty in measuring the extinction coefficient of the T–HMT furan-side monoadduct in the double-stranded M_{Fu}-A:B. The quantum yield can be estimated approximately by the using photo-cross-linking rate constant k^t_{XL} and the extinction coefficient of thee isolated T–HMT furan-side monoadduct. Though the error in the quantum yield so calculated is unknown, the data in Table III clearly indicate that the quantum yield for photo-cross-linking of M_{Fu}-A at wavelengths above 300 nm (2.4×10^{-2}) is much larger than the corresponding value for the photoreversal of the T–HMT furan-side monoadduct (7×10^{-4}, the preceding paper). The photoreversal of the single-stranded M_{Fu}-A above 300 nm is even less efficient than that of the T–HMT furan-side monoadduct (see the preceding paper). This explains why at wavelengths ≥313 nm only photo-cross-linking was observed.

The quantum yields of photo-cross-linking of M_{Fu}-A at wavelengths ≤281.7 nm are slightly larger than those at longer wavelengths. This difference could be due to either more

efficient cross-linking of the monoadduct at these wavelengths or energy transfer from excited DNA bases to the HMT group in the monoadduct, especially around 260 nm, where DNA bases absorb efficiently. At wavelengths above 300 nm, DNA bases absorb little light, and only the absorption of the T–HMT furan-side monoadduct in the helix contributes to the photo-cross-linking. The quantum yield at wavelengths above 300 nm is similar to that observed for the photo-cross-linking of the thymidine–8-methoxypsoralen furan-side monoadduct in calf thymus DNA (Tessman et al., 1985).

Enhanced Photoreversal of M_{Py}-A in Double-Stranded DNA. In contrast to M_{Fu}-A:B, UV irradiation of double-stranded M_{Py}-A:B results mostly in photoreversal of M_{Py}-A. Consequently, the photoreaction rate constant approximates the value of the photoreversal rate constant of M_{Py}-A in the double helix. Results show that photoreversal of M_{Py}-A in the double helix is more efficient than that in the single-stranded helix. Upon the formation of the double-stranded M_{Py}-A:B, the electronic and steric constraints of the T–HMT pyrone-side monoadduct may change, thereby affecting the photoreversal of the monoadduct. As described above, energy transfer from excited DNA bases in the double-stranded DNA to the HMT group may also play a role in the enhancement of photoreversal. Two other mechanisms, though having only a small effect as described above, can also contribute to the enhanced photoreversal. These are photoreversal through a transient cross-link formation and direct photoisomerization. In the first case, the cross-link is formed initially and then photoreversed. Approximately 70% of the photoreversal of the cross-link will produce the furan-side monoadducted B and unmodified oligonucleotide A (Cimino et al., 1986), consequently increasing the apparent photoreversal rate constant of M_{Py}-A. In the second case, the excited HMT group photoreverses at the pyrone end and simultaneously attaches to B through its furan end. This yields the same products as in the first case.

CONCLUSIONS

In this paper we have shown that the photoreactions of the HMT-monoadducted oligonucleotide in the double-stranded state are quite different from that in the single-stranded state. In the case of the pyrone-side monoadducted oligonucleotide, M_{Py}-A, photoreversal is the predominant reaction even in a double helix, and very little cross-link is generated. The photoreversal of the monoadduct in the double-stranded DNA is enhanced compared to that in the single-stranded DNA. In contrast, UV irradiation of M_{Fu}-A in the double-stranded state produces predominantly cross-link, although the amount of cross-link decreases after prolonged irradiation at wavelengths $\leq$313 nm due to photoreversal of the cross-link. At wavelengths $\geq$313 nm, no photoreversal of M_{Fu}-A can be detected, and photo-cross-linking occurs with a quantum yield of 2.4×10^{-2}.

ACKNOWLEDGMENTS

We thank Dr. G. D. Cimino, Dr. H. Gamper, and J. D. Kahn for helpful discussions and critical comments on the manuscript.

REFERENCES

Bensasson, R. V., Salet, C., Land, E. J., & Rushton, F. A. P. (1980) *Photochem. Photobiol. 31*, 129–133.

Blais, J. Ronfard-Haret, J. C., Vigny, P., Cadet, J., & Voituriez, L. (1985) *Photochem. Photobiol. 42*, 599–602.

Cimino, G. D., Gamper, H. B., Isaacs, S. T., & Hearst, J. E. (1985) *Annu. Rev. Biochem. 54*, 1151–1193.

Cimino, G. D., Shi, Y.-B., & Hearst, J. E. (1986) *Biochemistry 25*, 3013–3020.

Gasparro, F. P., Saffran, W. A., Cantor, C. R., & Edelson, R. L. (1984) *Photochem. Photobiol. 40*, 215–219.

Land, E. J., & Truscott, T. G. (1979) *Photochem. Photobiol. 29*, 861–866.

Maniatis, T., Fritsch, E. F., & Sambrook, J. (1982) in *Molecular Cloning*, pp 125–127, Cold Spring Harbor Laboratory, Cold Spring Harbor, NY.

Parsons, B. J. (1980) *Photochem. Photobiol. 32*, 813–821.

Shi, Y., & Hearst, J. E. (1986) *Biochemistry 25*, 5895–5902.

Shi, Y., & Hearst, J. E. (1987) *Biochemistry* (preceding paper in this issue).

Song, P. S., & Tapley, K. J., Jr. (1979) *Photochem. Photobiol. 29*, 1177–1197.

Tessman, J. W., Isaacs, S. T., & Hearst, J. E. (1985) *Biochemistry 24*, 1669–1676.